International Telecommunication Union

ITU-R

Radiocommunication Sector of ITU

Report ITU-R S.2362-0

(06/2015)

Methodology to estimate the sensitivity of GSO FSS interference levels to the geographical location of earth stations communicating with GSO satellites in the fixed-satellite service in the 14 GHz and 30 GHz frequency ranges

S Series

Fixed satellite service

150 1865-2015

ITU International Telecommunication Union

Foreword

The role of the Radiocommunication Sector is to ensure the rational, equitable, efficient and economical use of the radio-frequency spectrum by all radiocommunication services, including satellite services, and carry out studies without limit of frequency range on the basis of which Recommendations are adopted.

The regulatory and policy functions of the Radiocommunication Sector are performed by World and Regional Radiocommunication Conferences and Radiocommunication Assemblies supported by Study Groups.

Policy on Intellectual Property Right (IPR)

ITU-R policy on IPR is described in the Common Patent Policy for ITU-T/ITU-R/ISO/IEC referenced in Annex 1 of Resolution ITU-R 1. Forms to be used for the submission of patent statements and licensing declarations by patent holders are available from http://www.itu.int/ITU-R/go/patents/en where the Guidelines for Implementation of the Common Patent Policy for ITU-T/ITU-R/ISO/IEC and the ITU-R patent information database can also be found.

Series of ITU-R Reports

(Also available online at http://www.itu.int/publ/R-REP/en)

Series	Title
BO	Satellite delivery
BR	Recording for production, archival and play-out; film for television
BS	Broadcasting service (sound)
BT	Broadcasting service (television)
F	Fixed service
M	Mobile, radiodetermination, amateur and related satellite services
P	Radiowave propagation
RA	Radio astronomy
RS	Remote sensing systems
S	**Fixed-satellite service**
SA	Space applications and meteorology
SF	Frequency sharing and coordination between fixed-satellite and fixed service systems
SM	Spectrum management

***Note**: This ITU-R Report was approved in English by the Study Group under the procedure detailed in Resolution ITU-R 1.*

Electronic Publication
Geneva, 2015

REPORT ITU-R S.2362-0

Methodology to estimate the sensitivity of GSO FSS interference levels to the geographical location of earth stations communicating with GSO satellites in the fixed-satellite service in the 14 GHz and 30 GHz frequency ranges

(2015)

TABLE OF CONTENTS

Page

1 Introduction

A network of earth stations using the multi-frequency time-division multiple access (MF-TDMA) protocol can be used to provide high-data rate services over the geostationary-satellite orbit (GSO) fixed-satellite service (FSS). Methodologies to assess the interference from such networks were addressed in Recommendation ITU-R S.2029.

Interference from an earth station to a victim receiver in an adjacent satellite network depends on the location of the interfering earth station. Therefore, it is useful to investigate the sensitivity of interference to the location of an earth station. This Report investigates the effect of the location accuracy of the earth station for determining the interference levels onto an adjacent GSO FSS satellite network. The document considers a network of small aperture earth stations that operate using a TDMA protocol. Moreover, the earth stations may operate in the presence of antenna pointing errors. Because of the antenna pointing errors, the TDMA protocol, and the different e.i.r.p. spectral density levels of the earth stations, the proposed methodology is based on a statistical analysis. This methodology quantifies the sensitivity of the interference levels to the geographical locations of the interfering earth stations. This methodology is suitable for estimating the interference from a network of earth stations to victim earth terminals in the GSO FSS.

This Report is organized as follows. Section 2 describes the analysis approach and provides an overview of the methodology. Section 3 contains a detailed list of symbols used in this document. Section 4 discusses the statistical model for the analysis of interference; it describes the approach used for approximating the locations of the terminals; and it gives a methodology to obtain the cumulative distribution functions (CDFs) of the interference using the exact location, the approximate location, and next it determines the difference in the interference power spectral density (PSD). Section 5 presents some simulation results for satellite networks operating at the 30 GHz and 14 GHz frequency ranges. Section 6 discusses the applications of the methodology and section 7 provides the conclusions.

2 Overview of the methodology

The methodology described in this Report is based on a statistical analysis of the interference PSD that is received at a victim receiver of an adjacent satellite network. It assumes that all link parameters necessary to compute this interference PSD are available. However, the actual locations of the terminals are not available but they are approximated by a set of predetermined grid points as described below. The location "error" of a terminal is given by the difference between the actual location of the terminal and its approximated value. The interference PSD computed using these approximated location data of the terminals could be greater or less than its actual value resulting in, respectively, overestimation or underestimation of the interference PSD. The difference in interference PSD between the actual and the approximated location data is computed and with this information the CDF of the difference in the interference PSD as a function of the location error of the terminals is obtained. Furthermore, the difference in the interference PSD is examined as a function of the distance between adjacent grid points and the e.i.r.p. density of the terminals.

The specific steps used in this analysis are described as follows.

– Step 1. Compute the interference PSD to a victim receiver in an adjacent satellite network and estimate its CDF. This step makes use of the actual locations of the terminals and the relevant link parameters of the satellite networks.

– Step 2. Estimate the interference PSD using the approximated locations of the terminals. Quantize the spatial region where the terminals are operating to a finite set of grid points. These grid points may be determined a-priori. The spacing between adjacent points determines the accuracy of the location of the terminal.

– Step 2 (a). Approximate the location of each terminal to one of the grid points, preferably the nearest. The location error in this case is the difference between the actual location of the earth station and its approximated location to this grid point.

– Step 2 (b). Estimate the interference PSD and its CDF, assuming that the locations of the terminals are given by these approximated grid points.
Carry out this analysis for different e.i.r.p. density values of the earth station. This is necessary to examine the effect of the e.i.r.p. density level on the estimated interference using the approximated locations.

– Step 3. Determine the difference between the interference PSDs obtained using the actual locations of the terminals and their approximated locations. Estimate its CDF.

3 List of symbols

The symbols listed below are used in this Report:

$\beta_{i,r}$: angle at Satellite S_i between directions S_iC_i and S_iT_i.

$\beta_{v,r}$: angle at Satellite S_v between directions S_vC_v and S_vT_i.

γ_i : transmission gain from the output of receive antenna at Satellite S_i to output of receive antenna at R_v.

γ_v : transmission gain from the output of receive antenna at Satellite S_i to output of receive antenna at R_v.

ϕ: antenna pointing error at the interfering terminal.

ϕ_ϵ, ϕ_a: components of the antenna pointing error in the elevation and azimuth directions.

ψ: off-axis angle, measured from the antenna boresight direction, at T_i.

$\psi_{center,v}$: off-axis angle towards S_v at an interference terminal located at the beam center of S_v.

$\psi_{r,v}$: angle at T_i between its boresight direction and direction T_iS_v.

C_v, C_i : beam centers of Satellites S_v, S_i on the Earth.

$d(x_1, x_2)$: distance metric between points x_1 and x_2.

E_n: boresight e.i.r.p. spectral density of interfering terminal. $n = 1,2, \dots n_E$.

E_r: boresight e.i.r.p. spectral density at T_i located at r.

$E_r(\psi)$: e.i.r.p. spectral density in an off-axis angle ψ from T_i located at r.

E_{red}: reduction in boresight e.i.r.p. spectral density to account for underestimation of the actual interference when quantized locations are used.

G_v^s, G_i^s : receive antenna gain pattern at S_v, S_i.

I_{center}: interference power spectral density at the output of receive antenna of R_v due to a hypothetical interference terminal located at the beam center of S_v and transmitting at the ESD level specified by Recommendations ITU-R S.524-9 or S.728-1.

$I_{e,n,k}(r)$: difference between the interference power spectral densities when they are computed using the actual and approximated locations and when the transmit terminal is in the Region R_k with boresight e.i.r.p. spectral density E_n.

$I_i(r)$: interference power spectral density received via Satellite S_i at the output of receive antenna of R_v.

$I_{i,q}(r)$: interference power spectral density received via Satellite S_i at the output of receive antenna of R_v when spatial locations are quantized.

$I_v(r)$: interference power spectral density received via Satellite S_v at the output of receive antenna of R_v.

$I_{v,q}(r)$: interference power spectral density received via Satellite S_v at the output of receive antenna of R_v when spatial locations are quantized.

$L_{u,r}$: uplink loss from T_i located at r to satellites S_v or S_i.

n_E : number of different boresight e.i.r.p. spectral density levels.

p_{n,E_r} : probability that the interfering terminal at r is transmitting at boresight e.i.r.p. spectral density level E_n.

p_{n,k,E_r} : probability that an interfering terminal located in Region R*k* is transmitting at boresight e.i.r.p. spectral density level E_n.

p_r : probability that the interfering terminal at r is transmitting data.

p_{r_k}: probability that the transmit terminal is in Region R*k*.

r : spatial location variable of the interfering terminal that is transmitting data.

r_Δ: distance between adjacent grid points.

r_k : quantized values of r. $k = 1,2, \ldots K$.

R : spatial region where the interfering terminals are distributed.

R*k* : k^{th} quantization region.

R_v : victim receiver.

S_v, S_i : wanted and interfering satellites.

t_k : total time duration interfering terminals are transmitting from Region R*k*.

$t_{n,k}$: total time duration interfering terminals are transmitting from Region R*k* with boresight ESD level E_n.

T_v, T_i : wanted and interfering transmit terminals.

4 Model for the interference analysis

A graphical representation of the interference model is shown in Fig. 1. The transmit terminals of the interfering network are denoted by T_i. This figure also shows the victim and interfering satellites, S_v and S_i, wanted (victim) transmit terminal T_v, and victim receive terminal R_v. The spatial location of the Terminal T_i is denoted by the variable r, which is in general a three-dimensional variable corresponding to the spatial coordinates of that location. The interfering terminals use the multi-frequency (MF) time-division multiple access (TDMA) protocol with only a single terminal transmitting at a particular time instant in a narrow frequency band of interest. For modeling purposes, it is assumed that the Satellites S_v and S_i employ the same frequency translation from the uplink to the downlink. If this is not the case, the downlinks from S_v and S_i to R_v correspond to terminals from different interfering networks.

FIGURE 1

Interference paths from Terminal T_i to the victim receiver R_v, via Satellites S_i and S_v. C_i and C_v denote the beam centers of S_i and S_v on the Earth surface; O is the origin from which the distances to the terminal locations are measured

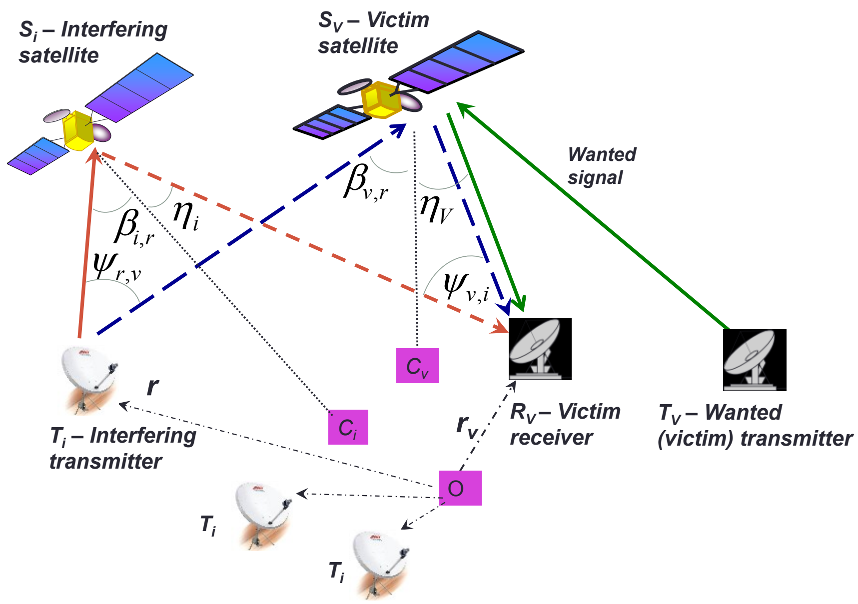

Further details of this interference model and methodologies to assess the interference are given in Recommendation ITU-R S.2029. The focus of this Report is on investigating the effect on the interference when the locations of the interfering terminals are approximated by a set of quantized values of r.

4.1 Statistical model for the terminal locations and their e.i.r.p. levels

In this analysis the interfering terminals of the earth station network transmit in a random manner, and in a given time instant only a single terminal transmits data. The location of this terminal is represented by the random variable r, and its probability density function (PDF) denoted by p_r. When all the interfering terminals are in a Region R, it follows that $\int_{\mathrm{R}} p_r(r)\, dr$. Observe that only the interfering terminal that transmits at a particular time instant is of interest and the location of this terminal is represented by r; the interfering terminals in the network that do not transmit at this time instant are not of interest from an interference standpoint.

For small aperture terminals, because of off-axis emission limits, the e.i.r.p. spectral density (ESD) in the boresight direction depends on the aperture size of the terminal's antenna. Consider a network of terminals consisting of n_E antenna aperture sizes that are distributed randomly. Then the distribution of the boresight ESD can be represented by a discrete probability distribution with values from the set $\{E_1, E_2, \ldots E_{n_E}\}$. The conditional PDF of the ESD, conditioned on the specific location r of the terminal, is given by the discrete probabilities $\{p_{1,E_r}, p_{2,E_r}, \ldots p_{n_E,E_r}\}$, where p_{n,E_r} is the probability that the terminal at r transmits with boresight ESD level E_n and $\sum_{n=1}^{n_E} p_{n,E_r} = 1$. Observe that with this formulation there could be multiple terminals at r with different boresight ESD levels; however, only a single terminal can transmit at a given time instant.

4.2 Interference signal using actual locations

The signal paths from the interfering terminals to the victim receiver via the interfering and victim satellites are shown Fig. 1. The interference power spectral densities (PSDs) at the victim receiver, via Satellites S_v and S_i, due to the interfering terminal T_i at r are denoted by $I_v(r)$ and $I_i(r)$, respectively. These can be expressed in terms of the satellite link parameters and γ_{v} and γ_{i}. Note that the downlink path transmission gains from the satellites are not functions of the specific locations of the interfering terminals. Therefore, the values of γ_v and γ_i do not change when the interference is evaluated by assuming that the locations of the transmit terminals are approximated by a set of quantized values of the location variable.

Using the satellite link parameters and notation listed in § 3, the interference power spectral densities received via Satellites S_v and S_i are expressed as

$$I_v(r) = \frac{E_r(\psi_{r,v})G_v^S(\beta_{v,r})}{L_{u,r}}\gamma_v$$
$$I_i(r) = \frac{E_r(0)G_i^S(\beta_{i,r})}{L_{u,r}}\gamma_i. \quad (1)$$

In the above it is assumed that the orbital separation between the satellites is close so that the uplink path losses to the satellites are the same. Note that the total interference PSD at the victim receiver is $(I_v(r) + I_i(r))$ and for high-gain receive antennas at the victim receiver $I_v(r) \gg I_i(r)$ because $\gamma_v \gg \gamma_i$. The analytical expressions for the CDFs of $I_v(r)$ and $I_i(r)$ can be determined using the PDFs of the random variables r and E_r. In the Annex, a step-by-step Monte-Carlo simulation process is given to calculate the CDFs of these interference PSD terms.

4.3 Interference estimated using quantized spatial locations

The locations of the interfering terminals are approximated by a set of grid points obtained by quantizing the location variable r. These quantized points are denoted by r_k, $k = 1,2, \dots K$, and R_k is the k^{th} quantization region, that is, all spatial locations within R_k are represented by the grid point r_k. An illustrative quantization scheme for the locations of the interfering terminals is shown in Fig. 2.

FIGURE 2

Quantization of Region R to Regions R_k, $k = 1, 2, . . . , K$. Representative centre of R_k is shown as r_k. The points "o" denote the specific locations of the interfering terminals. $E_n, n = 1, 2, \dots n_E$, denote the boresight e.i.r.p. density levels at these terminals

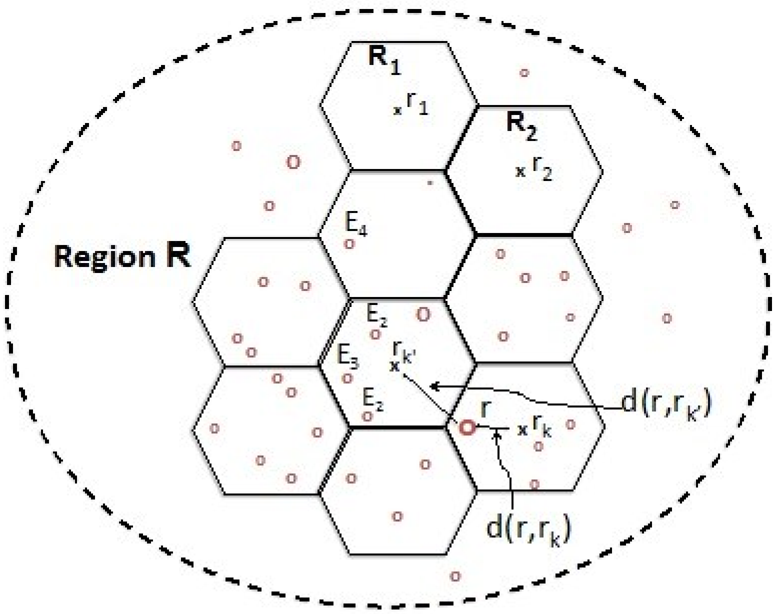

This Figure shows K quantized regions, R_1, R_2, . . . R_K. These quantized regions are disjoint and encompass the entire region of interest R. Note that although this Figure shows a regular pattern for the quantized regions, in general, they may take the shape of some conveniently chosen predetermined pattern. In this figure the actual locations of the interfering terminals are shown as "o" and these terminal locations are quantized to one of the points r_k, $k = 1,2, \dots K$, such that the quantized point is the nearest to the location of the terminal. Specifically, denote the distance metric between the interfering terminal located at r and a quantized point r_k as $d(r, r_k)$. Then this terminal is located in Region R$_k$ and represented by the grid point r_k when the following is satisfied

$$r \in R_k \quad \text{if } d(r, r_k) \le d(r, r_{k'}),\ r_k \ne r_{k'}. \tag{2}$$

In the simulations presented later the Euclidean distance metric is considered for the function $d(x_1, x_2)$, which is the distance between the two points x_1 and x_2.

The interference is now computed assuming that the interfering terminals are located at the representative points r_k rather than at their actual locations r. Specifically, the interfering terminal at r with boresight ESD E_r is relocated to r_k. So the resulting interference PSDs corresponding to $I_v(r)$ and $I_i(r)$ in equation (1) are expressed as

$$\begin{aligned} I_{v,q}(r_k) &= \frac{E_r\left(\psi_{r_k,v}\right) G_v^S\left(\beta_{v,r_k}\right)}{L_{u,r_k}} \gamma_v \\ I_{i,q}(r_k) &= \frac{E_r(0) G_i^S\left(\beta_{i,r_k}\right)}{L_{u,r_k}} \gamma_i. \end{aligned} \tag{3}$$

The link parameters on the right-hand side of the above equation are with respect to the quantized locations r_k. The variables, $\psi_{r_k,v}$, $G_v^S\left(\beta_{v,r_k}\right)$, $G_i^S\left(\beta_{i,r_k}\right)$ and L_{u,r_k} can be determined by using their respective values at the grid point, r_k. The boresight ESD E_r is a random variable and it is the same value as that of the corresponding terminal located at the actual location r.

4.3.1 Statistics of r_k and E_r in quantized regions

Estimating the PDFs of the random variables r_k and E_r is described next. Denote by $p_{r_k} = \text{Prob}\{r \in \text{R}_k\}$, which is the probability that the transmit terminal is in the Region R$_k$. This probability can be expressed as:

$$p_{r_k} = \int_{r \in R_k} p_r\,(r) dr \tag{4}$$

Note that $\sum_{k=1}^{K} p_{r_k} = 1$. When the PDF p_r is known these probabilities can be determined for a given set of quantization regions. On the other hand, these probabilities can also be estimated using the method of relative frequency of occurrence of the terminals in the respective quantization regions. For example, suppose t_k is the total time interval the terminals are transmitting from the Region R$_k$, then

$$p_{r_k} = \frac{t_k}{\sum_{i=1}^{K} t_i} \tag{5}$$

Next, E_r takes values from the set $\{E_1, E_2, \dots E_{n_E}\}$ and the desired probability is $p_{n,k,E_r} = \text{Prob}\{E_r = E_n | r \in \text{R}_k\}$, that is the probability that the boresight ESD of the transmit terminal is E_n when it is transmitting from Region R$_k$. This probability can be determined analytically when the PDFs p_r and p_{n,E_r} are known. Alternatively, the following method could be used to estimate this PDF. This method requires tabulating the time duration of occurrence of each ESD level at each Region R$_k$ in the desired observation time interval. Denote by $t_{n,k}$ the time duration for which the ESD E_n is used in the Region R$_k$. Then the desired PDF is estimated as

$$p_{n,k,E_r} = \frac{t_{n,k}}{\sum_{i=1}^{n_E} t_{i,k}} \tag{6}$$

The CDFs of the interference terms $I_{v,q}(r_k)$ and $I_{i,q}(r_k)$ given in equation (3) can be determined using the above PDFs. A Monte-Carlo simulation method to estimate these CDFs is given in the Annex.

4.4 The difference between the interference PSDs

The interference PSDs using the actual locations of the terminals are given by $I_v(r)$ and $I_i(r)$ in equation (1). The corresponding interference PSDs when the locations are approximated by the grid points r_k are given by $I_{v,q}(r_k)$ and $I_{i,q}(r_k)$ in equation (3). The difference in the interference PSD is because the actual locations of the terminals are approximated by the grid points. In order to determine this difference, first consider a terminal with a boresight ESD level E_n at r. The corresponding interference PSDs can be obtained from equation (1) by setting $E_r = E_n$. Observe that this event occurs with probability p_{n,E_r}. The location of this terminal, r, is now quantized to the grid point r_k and the corresponding interference PSDs are obtained from equation (3) by replacing E_r with E_n. The difference between the interference PSDs is the "error" in the interference PSD and occurs with probability p_{n,E_r}.

This difference term can be expressed as:

$$I_{e,n,k}(r) = \left(\frac{E_n(\psi_{r,,v})G_v^S(\beta_{v,r})}{L_{u,r}} - \frac{E_n\left(\psi_{r_k,v}\right)G_v^S\left(\beta_{v,r_k}\right)}{L_{u,r_k}}\right)\gamma_v + \left(\frac{E_n(0)G_i^S(\beta_{i,r})}{L_{u,r}} - \frac{E_n(0)G_i^S\left(\beta_{i,r_k}\right)}{L_{u,r_k}}\right)\gamma_i. \quad (7)$$

The CDF of $I_{e,n,k}(r)$ can be computed using the PDFs of the underlying random variables r and E_r. In the simulations given in § 5, a Monte-Carlo method is used to evaluate the CDF of this difference between the interference PSDs.

Note the following two cases:

$I_{e,n,k}(r) < 0$, the interference PSD estimated using the approximated locations is more than the actual interference PSD and it overestimates the actual interference PSD;

$I_{e,n,k}(r) > 0$, the interference PSD estimated using the approximated locations is less than the actual interference PSD and it underestimates the actual interference PSD.

Observe that by reducing the boresight ESD of the terminals, that is E_n in the first and third terms on the right-hand side of equation (7), this underestimation error can be reduced. Section 5 presents simulation results to study this effect.

4.5 Interference PSD in the presence of antenna pointing errors

Methodologies to account for the effects of antenna pointing errors in the interference PSD are addressed in Recommendations ITU-R S.1857 and ITU-R S.2029. The antenna pointing error, ϕ, is defined as the angle between the boresight direction of the interfering terminal's antenna and the desired direction to the satellite. The antenna pointing error is usually measured in terms of its components: the errors in the elevation and azimuth directions, which are denoted by ϕ_ε and ϕ_a, respectively. Recommendation ITU-R S.1857 describes the method to compute ϕ using the observations ϕ_ε and ϕ_a. Modifying (1) to account for the antenna pointing errors, the interference PSDs due to a terminal at r with an antenna pointing error of ϕ is

$$I_v(r,\phi) = \frac{E_r\left(\psi_{r,v}(\phi)\right)G_v^S(\beta_{v,,r})}{L_{u,r}}\gamma_v$$
$$I_i(r,\phi) = \frac{E_r(\phi)G_i^S(\beta_{i,r})}{L_{u,r}}\gamma_i \quad (8)$$

where the off-axis angle is shown as a function of ϕ. When r is quantized to the grid point r_k the terminal with boresight ESD E_r is relocated to r_k. The antenna pointing error at this terminal is the same at both r and r_k. Modifying equation (3) to account for the antenna pointing errors, the interference PSDs estimated using the grid points is

$$I_{v,q}(r_k, \phi) = \frac{E_r\left(\psi_{r_k,v}(\phi)\right) G_v^S\left(\beta_{v,r_k}\right)}{L_{u,r_k}} \gamma_v$$
$$I_{i,q}(r_k, \phi) = \frac{E_r(\phi) G_i^S\left(\beta_{i,r_k}\right)}{L_{u,r_k}} \gamma_i. \tag{9}$$

Finally, the difference between the interference PSDs can be computed using equations (8) and (9). In the results presented in the next section computer simulation examples are given for these interference PSDs and the difference between the interference PSDs.

5 Simulation results

This section presents some illustrative simulation results for satellite networks operating at the 30 GHz and 14 GHz frequency ranges.

5.1 Results at 30 GHz

In these simulations the terminals are distributed as shown in Fig. 3; the corresponding link parameters are given in Table 1. The beam pattern at the victim satellite corresponds to a narrow spot beam. This figure show the 6 dB contour of the receive antenna beam. Distribution-A, shown in Fig. 3, is a two-dimensional distribution centered at Washington, D.C.

FIGURE 3

Distribution-A of Terminals T_i and the 6-dB contour of receive antenna beam of Satellite S_v.
The beam center of S_v is at Harrisburg, Pennsylvania. This shows a set of grid points within Region R

TABLE 1

Satellite link parameters used with terminal Distribution-A in Fig. 3

Uplink frequency	29.75 GHz
Aperture diameters of T_i	(0.2, 0.25, 0.3, 0.35, 0.4) m uniformly distributed
Antenna pointing errors at T_i, ϕ_ε and ϕ_a	independent and identically distributed normal random variables with mean zero and variance 0.2 degrees
Locations of T_i, Distribution-A	uniformly distributed within a circular area centered at Washington, D.C. with a radius of 70 km
Longitudes at Satellites S_v, S_i	102.8^0 W and 100.2^0 W
Locations of C_v, C_i: (latitude, longitude)	Harrisburg, Pennsylvania. (41.27^0 N, 76.88^0 W)
Receive antennas at satellites	1.4 m diameter aperture with parabolic illumination and efficiency 0.55

The grid points for Distribution-A form a square grid within the Region R with distance between adjacent grid points, $r_\Delta = (r_k - r_{k-1})$, set to a constant value. In the simulations the effect of different values of r_Δ on the interference is examined.

The boresight ESD of the terminals are determined so that they transmit at the maximum level subject to the ESD level $(\text{Ka}_{\text{Mask}} - E_{\text{red}})$ dB(W/Hz), where Ka_{Mask} is the ESD level established in *recommends* 4 of Recommendation ITU-R S.524-9 and E_{red} is a small value to reduce the ESD levels to accommodate the underestimation of the interference PSD when quantized locations are used. Note that E_{red} is used only with the first and third terms on the right-hand side of equation (7).

Also, note that the ESD level $(\text{Ka}_{\text{Mask}} - E_{\text{red}})$ is satisfied by the terminals in the absence of antenna pointing errors; the boresight ESD was not reduced to account for the antenna pointing errors. These simulations considered a large aperture receive antenna at the victim terminal. Therefore, the terms $I_i(r)$ and $I_{i,q}(r_k)$ in equations (1) and (3) are ignored.

In order to normalize the interference PSDs consider a hypothetical terminal located at the beam center of Satellite S_v and assume that this terminal is transmitting at its maximum off-axis emission level given in Ka_{Mask}, which is $\left(19 - 25\log_{10}\psi_{center,v}\right)$ dB(W/40 kHz) where $\psi_{center,v}$ $\left(2^0 \leq \psi_{center,v} < 7^0\right)$ is the off-axis angle toward S_v in degrees. Denote by I_{center} the interference PSD from this terminal. Note that I_{center} is the maximum value of the interference PSD for any terminal location and any antenna aperture size.

Figure 4 shows the complementary CDFs of the normalized interference values $I_v(r)/I_{\text{center}}$ (without quantization) and $I_{v,q}(r_k)/I_{\text{center}}$ for the terminal Distribution-A, shown in Table 1.

For $I_{v,q}(r_k)/I_{\text{center}}$ the results are for r_Δ=20 and 50 km. It can be seen that when the boresight ESD of the terminals are not reduced, that is when E_{red}= 0 dB, there is very little difference in the interference PSDs. On the other hand, when E_{red}= 0.2 dB the interference PSD computed using the actual locations decreases. Because the interference PSD with quantized locations is more than the actual interference this results in overestimation of the actual interference PSD.

FIGURE 4

Complementary CDFs of the normalized interference PSDs for the Distribution-A shown in Table 1 $E_{red} = 0$ dB (top figure) and $E_{red} = 0.2$ dB (bottom figure). Legend shows values of r_Δ

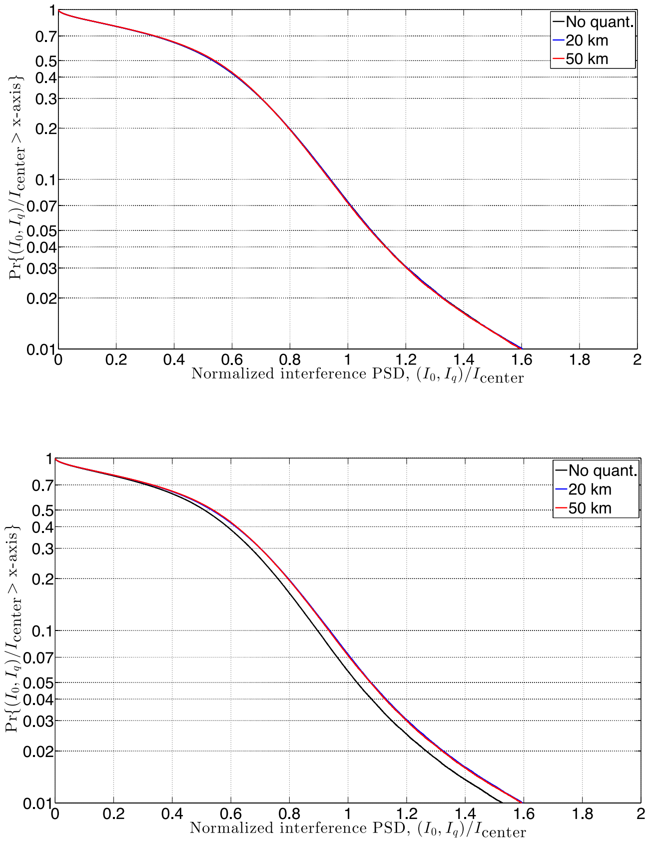

The CDF of the normalized difference between the interference PSDs, $I_{e,n,k}(r)/I_{center}$, for terminal Distribution-A is shown in Fig. 5. These results are for different values of r_Δ and E_{red}. Unlike the results in Fig. 4, these results show that the error is noticeable even when $E_{red} = 0$ dB. As expected the error in the interference PSD increases for larger values of r_Δ. For example, probability that $\frac{I_{e,n,k}(r)}{I_{center}} < 0.02$ is 0.9 when $E_{red} = 0$ dB and for r_Δ=20 km.

For the same probability, this error reduces to $\frac{I_{e,n,k}(r)}{I_{center}} < -0.0004$ when $E_{red} = 0.2$ dB. Note that $I_{e,n,k}(r) > 0$ corresponds to underestimation of the actual interference PSD and these results show that the underestimation of the actual interference PSD can be substantially reduced by slightly reducing the boresight ESD of the terminals. Fig. 6 shows Prob $\left\{\frac{I_{e,n,k}(r)}{I_{center}} < 0\right\}$, which is the probability of overestimating the actual interference PSD, as a function of E_{red}. As expected it can be seen that this probability increases with increasing values of E_{red}.

FIGURE 5

CDF of the difference between the interference PSDs for Distribution-A shown in Table 1
Legend shows r_{Δ} and E_{red}

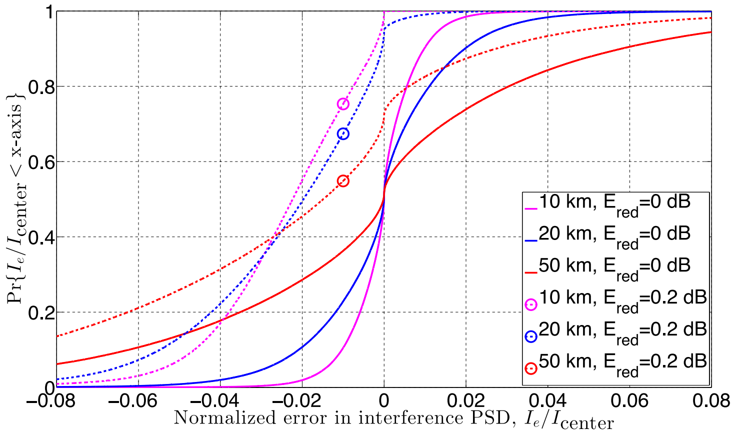

FIGURE 6

Prob $\left\{\frac{I_{e,n,k}(r)}{I_{center}} < 0\right\}$ as a function of E_{red} for Distribution-A shown in Table 1. Legend shows r_{Δ}

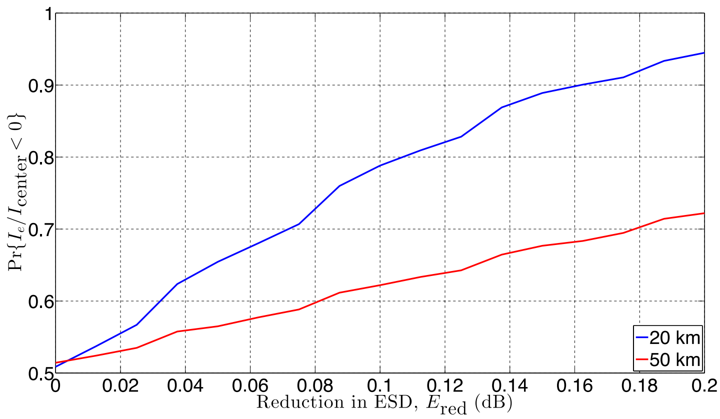

5.2 Results at 14 GHz

The results given in the preceding subsection are for a narrow spot beam antenna in the 30 GHz frequency range. In this subsection a wide beam receive antenna in a Ku-band satellite is considered. The 6 dB contour of the receive antenna beam of the victim satellite and the distribution of the terminals is shown in Fig. 7. Here the terminals are uniformly distributed (Distribution-B) in a region centered at Atlanta, Georgia and with radius 300 km. Table 2 shows the link parameters used in these simulations. The ESD levels of the terminals in this case comply with $(\mathrm{Ku_{Mask}} - E_{\mathrm{red}})$ dB(W/Hz), where $\mathrm{Ku_{Mask}}$ is the ESD level established in Recommendation ITU-R S. 728-1. Also, I_{center} corresponds to the ESD level $\mathrm{Ku_{Mask}}$ and the beam center of this antenna pattern is shown in Fig. 7. Note that, as in the results for the 30 GHz range, E_{red} is used only with the first and third terms on the right-hand side of equation (7).

FIGURE 7

Distribution-B of Terminals T_i and the 6-dB contour of receive antenna beam of Satellite S_v. The beam center of S_v is at Lexington, Kentucky

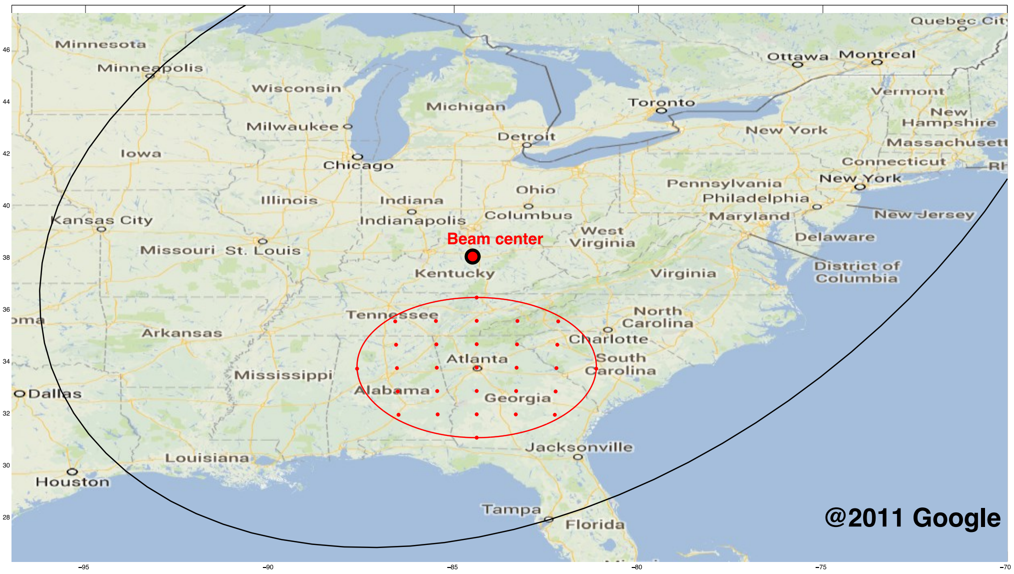

TABLE 2

Satellite link parameters used with the terminal distribution in Fig. 7

Uplink frequency	14.25 GHz
Aperture diameters of T_i	(0.3, 0.35, 0.4, 0.45, 0.5) m, uniformly distributed
Antenna pointing errors at T_i, ϕ_ε and ϕ_a	independent and identically distributed normal random variables with mean zero and variance 0.2^0
Locations of T_i, Distribution-B	uniformly distributed within a circular area centered at Atlanta, Georgia with a radius of 300 km
Longitudes at Satellites S_v, S_i	102.8^0 W and 100.2^0 W
Locations of C_v, C_i: (latitude, longitude)	Lexington, Kentucky. (38.03^0 N, 84.5^0 W)
Receive antennas at satellites	0.7 m diameter aperture with parabolic illumination and efficiency 0.55

Figure 8 shows the complementary CDFs of $I_v(r)/I_{\text{center}}$ (without quantization) and $I_{v,q}(r_k)/I_{\text{center}}$ for the terminal Distribution-B shown in Fig. 7 and the link parameters in Table 2. As seen from this figure when $E_{\text{red}} = 0.2$ dB there is a noticeable difference between the actual interference and the interference estimated using the approximated locations. Observe that r_Δ for these results are 100 km and 150 km. This is because, for a wide beam antenna at the victim satellite, the change in the satellite antenna gain pattern for these distances is very small.

FIGURE 8

Complementary CDFs of the normalized interference PSDs for the Distribution-B shown in Table 2 $E_{\text{red}} = 0$ dB (top figure) and $E_{\text{red}} = 0.2$ dB (bottom figure). Legend shows values of r_Δ

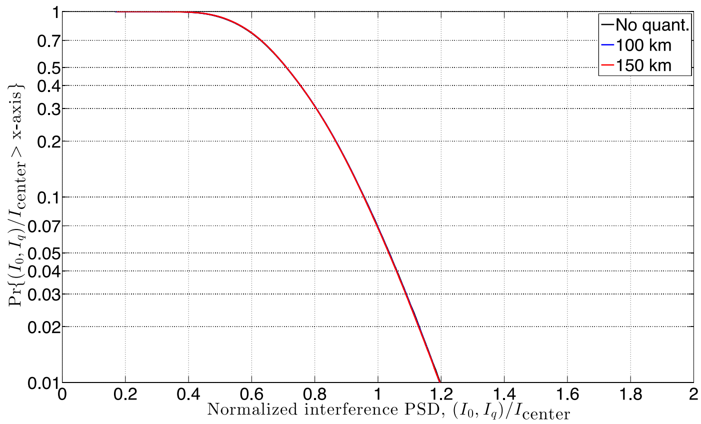

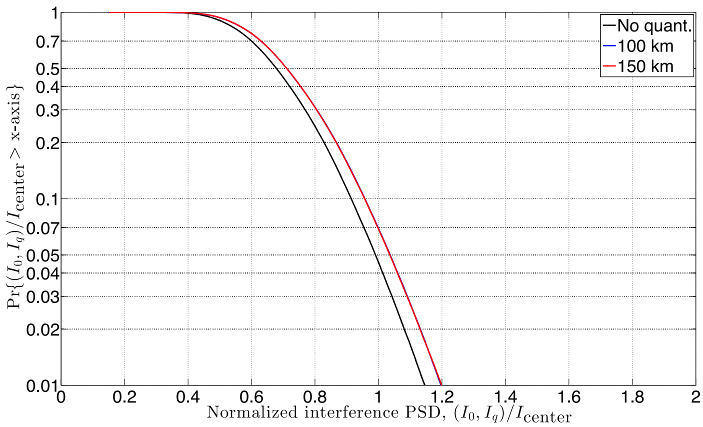

Figures 9 and 10 show the variations of the normalized error in the interference PSD for different values of E_{red} and r_Δ. As in the case for the narrow spot beam antenna, it can be seen that the probability of underestimating the actual interference can be reduced by slightly reducing the boresight ESD of the terminals.

FIGURE 9

CDF of the difference between the interference PSDs for Distribution-B shown in Table 2 Legend shows r_Δ and E_{red}

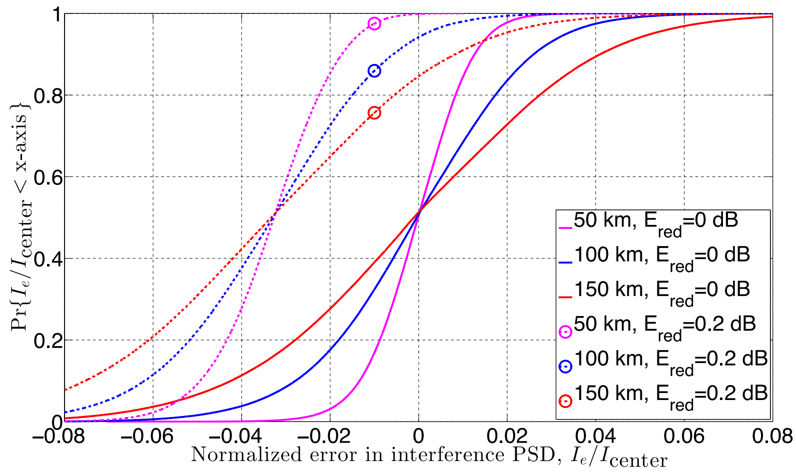

FIGURE 10

Prob $\left\{\frac{I_{e,n,k}(r)}{I_{\text{center}}} < 0\right\}$ as a function of E_{red} for Distribution-B shown in Table 2. Legend shows r_Δ

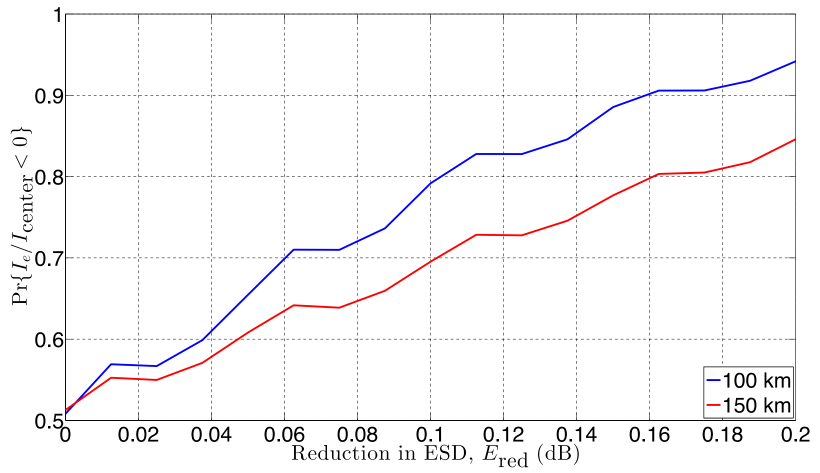

6 Discussion

The methodology presented in this Report allows the evaluation of interference from a network of earth stations operating with GSO FSS networks by using approximate locations, i.e. selected grid points within a grid. The results in Figs 5 and 9 show that the distance between grid points determines the accuracy of the estimation of interference using the approximate locations. It follows from these results that there is an imperceptible difference when the distances are small (no quantization, 100 m or 1 km) and the difference is noticeable only when the separation between grid points becomes larger, for example, 20 km at 30 GHz or 50 km at 14 GHz.

The results also show that by slightly reducing the e.i.r.p. levels of the transmit terminals the underestimation of the actual interference can be significantly reduced. Hence, the e.i.r.p. levels of the terminals can be reduced to guarantee that the actual interference is less than the estimated interference for a given probability level.

Therefore, in situations where it is not possible to provide the actual location of terminals with a high resolution, an alternative approach would be to provide the grid characteristics of the quantized region (e.g. size, grid-point separation, location within the satellite beam, etc.) and the associated distribution of the earth stations at these grids points and their e.i.r.p. distribution.

A step-by-step process included in the Annex shows how to use this information to obtain the interference values with a certain probability.

7 Conclusion

This Report presents a statistical methodology to estimate interference levels from an earth station network onto GSO FSS networks, based on approximate location information (latitude, longitude) of the terminals. The sample simulation results show the sensitivity of terminal location information to the resulting interference. Furthermore, the results show that approximated location values, within a certain range, i.e. not the actual locations, can provide reasonably good estimates of the actual interference.

Annex

A step-by-step method to estimate the interference PSDs

This Annex gives a step-by-step Monte-Carlo simulation method to estimate the interference PSDs using the actual locations and their approximated locations. Also, it shows how to estimate the difference in these interference PSDs.

It is assumed that $\gamma_v \gg \gamma_i$ so only the interference arriving via Satellite S_v is considered. Also, antenna pointing errors are not considered here.

1 Estimating the interference PSD using the actual locations

Input to the estimation process

N_r, number of actual locations of the terminals in the Region R.

Longitudes at Satellites S_v and S_i; location of the beam center of S_v, r_{center}; uplink frequency; and receive antenna gain pattern of S_v, G_v^S.

p_r, PDF of the locations of the terminals; and p_{n,E_r}, probability that the terminal at r is transmitting at boresight e.i.r.p. spectral density level E_n.

Estimation process

Step 1: Using the PDF p_r generate the $1 \times N_r$ location vector $\boldsymbol{\rho} = [\rho_1, \rho_2, \ldots \rho_{N_r}]$. This vector represents the actual locations, r, of the interfering terminals.

Step 2: Use the locations of the Satellites S_v and S_i and the location vector $\boldsymbol{\rho}$, to compute the off-axis angle $1 \times N_r$ vector to S_v, $\boldsymbol{\psi} = \left[\psi_{\rho_1,v}, \psi_{\rho_2,v}, \ldots \psi_{\rho_{N_r},v}\right]$.

Step 3: Using $\boldsymbol{\rho}$ and longitude and the beam center of S_v compute the angles $\beta_{v,\rho_1}, \beta_{v,\rho_2}, \ldots \beta_{v,\rho_{N_r}}$. Then the $1 \times N_r$ antenna gain pattern of S_v is $\mathbf{G} = \left[G_v^S(\beta_{v,\rho_1}), G_v^S(\beta_{v,\rho_1}), \ldots G_v^S\left(\beta_{v,\rho_{N_r}}\right)\right]$.

Step 4: The path losses from the terminal locations $\boldsymbol{\rho}$ to the Satellite S_v can be computed using longitude at S_v and the uplink frequency. This $1 \times N_r$ path loss vector is expressed as

$$\mathbf{L} = \left[L_{u,\rho_1}, L_{u,\rho_2}, \ldots L_{u,\rho_{N_r}}\right].$$

Step 5: The probability of occurrence of the boresight ESD level E_n at a given location ρ_i is given by $p_{n,E_{\rho_i}}$. The off-axis ESD vector at all the locations is

$$\mathbf{E}^{n}(\boldsymbol{\psi}) = \left[E_n(\psi_{\rho_1,v})p_{n,E_{\rho_1}}, E_n(\psi_{\rho_2,v})p_{n,E_{\rho_2}}, \ldots E_n\left(\psi_{\rho_{N_r},v}\right)p_{n,E_{\rho_{N_r}}}\right].$$

Step 6: The interference PSD due to a terminal at r and ESD level E_n can be computed using (1). The $1 \times N_r$ interference PSD vector due to terminals at $\boldsymbol{\rho}$ with ESD level E_n is

$$\mathbf{I}^{n} = \frac{\mathbf{E}^{n}(\boldsymbol{\psi}) \times \mathbf{G}}{\mathbf{L}} \gamma_v,$$

where the multiplication and division of the vectors is defined such that the i^{th}-element of $\mathbf{I}^{n}$, $(\mathbf{I}^{n})_i = \frac{(\mathbf{E}^{n}(\boldsymbol{\psi}))_i \times (\mathbf{G})_i}{(\mathbf{L})_i} \gamma_v$.

Step 7: Consider the interference PSD for all n_E ESD levels. The $1 \times (N_r \times n_E)$ interference PSD vector is $\mathbf{I} = [\mathbf{I}^{1}, \mathbf{I}^{2}, \ldots \mathbf{I}^{n_E}]$.

Step 8: Normalize $\mathbf{I}$ with respect to I_{center}. Using r_{center} determine the angle $\psi_{\text{center},v}$. The off-axis ESD level from this hypothetical terminal is $E_{\text{Mask}}(\psi_{\text{center},v})$ where $E_{\text{Mask}}(\psi)$ is the off-axis ESD levels specified in Recommendations ITU-R S.524-9 or ITU-R S.728-1.

Then $I_{\text{center}} = \frac{E_{\text{Mask}}(\psi_{\text{center},v}) G_v^s(0)}{L_{u,r_{\text{center}}}} \gamma_v$. The normalized interference PSD is $\mathbf{I}/I_{\text{center}}$, which does not contain the term γ_v.

Step 9. Estimate the CDF of $\mathbf{I}/I_{\text{center}}$.

2 Estimating the interference PSD using the grid points

Additional input to the estimation process

$1 \times K$ vector of grid points $\mathbf{r_k} = [r_1, r_2, \ldots r_K]$.

Estimation process

Step 1: Using $\mathbf{r_k}$ determine the $1 \times K$ vectors $\mathbf{G_k} = [G_v^s(\beta_{v,r_1}), G_v^s(\beta_{v,r_2}), \ldots G_v^s(\beta_{v,r_k})]$, $\mathbf{L_k} = [L_{u,r_1}, L_{u,r_2}, \ldots L_{u,r_k}]$, and $\boldsymbol{\psi}_\mathbf{k} = [\psi_{r_1,v}, \psi_{r_2,v}, \ldots \psi_{r_k,v}]$.

Step 2: Quantize each element of $\boldsymbol{\rho}$ to the nearest point in $\mathbf{r_k}$. Construct this $1 \times N_r$ quantized vector of $\boldsymbol{\rho}$, $\boldsymbol{\rho}_q = [\rho_{q,1}, \rho_{q,2}, \ldots \rho_{q,N_r}]$, where $\rho_{q,i} = r_k$ when $\rho_i \in \mathrm{R_k}$. Note that the elements of $\boldsymbol{\rho}_q$ are $r_k, k = 1,2, \ldots K$. Denote the mapping of the elements from $\mathbf{r_k}$ to $\boldsymbol{\rho}_q$ by $\mathbf{Q}$. That is $\boldsymbol{\rho}_q = \mathbf{Q}(\mathbf{r_k})$.

Step 3: Apply the mapping $\mathbf{Q}$ to the $1 \times K$ vectors in Step 1 to rearrange the terms to $1 \times N_r$ vectors and denote them by $\mathbf{G_q} = \mathbf{Q}(\mathbf{G_k})$, $\mathbf{L_q} = \mathbf{Q}(\mathbf{L_k})$ and $\boldsymbol{\psi}_\mathbf{q} = \mathbf{Q}(\boldsymbol{\psi}_\mathbf{k})$.

Step 4: The $1 \times N_r$ off-axis ESD vector is obtained by replacing the off-axis angle, with that corresponding to the quantized locations, in the off-axis ESD level given in Step 5 of the preceding section. The resulting off-axis ESD vector is

$$\mathbf{E}_q^{n}(\boldsymbol{\psi}) = \left[E_n(\psi_{q,1})p_{n,E_{\rho_1}}, E_n(\psi_{q,2})p_{n,E_{\rho_2}}, \ldots E_n(\psi_{q,N_r})p_{n,E_{\rho_{N_r}}}\right],$$

where $\psi_{q,i}$ is the i^{th}- element of $\boldsymbol{\psi}_\mathbf{q}$.

Step 5: The $1 \times N_r$ interference PSD vector due to quantized locations and boresight ESD level E_n is

$$\mathbf{I}_q^n = \frac{\mathbf{E}_q^n(\boldsymbol{\psi}) \times \mathbf{G}_q}{\mathbf{L}_q} \gamma_v.$$

Step 6: Form the $1 \times (n_E \times N_r)$ interference PSD vector due to all the E_n levels $\mathbf{I}_q = [\mathbf{I}_q^1, \mathbf{I}_q^2, \dots \mathbf{I}_q^{n_E}]$.

Step 7: Estimate the CDF of the normalized vector, $\mathbf{I}_q / I_{\text{center}}$.

Step 8: The normalized error in the interference PSDs is $(\mathbf{I} - \mathbf{I}_q) / I_{\text{center}}$. Estimate its CDF.